Calculation of the Inelastic Scanning Tunneling Image of Acetylene on Cu(100)

N. Mingo* and K. Makoshi
Faculty of Science, Himeji Institute of Technology, Kamigori, Ako-gun, Hyogo 678-1297, Japan
(Received 26 August 1999)

A Green function linear combination of atomic orbitals technique is used to theoretically calculate the "inelastic" scanning tunneling microscope image of a C_2H_2 molecule adsorbed on Cu(100) and explain previous experimental results. Our analysis of the inelastic scattering process in terms of the orbitals shows that a destructive interference occurs in the inelastic scattering by the C-H bending modes. This results in a much smaller inelastic fraction due to the bending modes as compared to the stretching ones, and explains why the former cannot be observed experimentally.

PACS numbers: 73.40.Gk, 61.16.Ch, 68.35.Ja, 82.65.Pa

Inelastic tunneling spectroscopy of molecules in an interface has been known for several decades [1]. However, only very recently it has become possible to perform inelastic tunneling experiments with a scanning tunneling microscope (STM) [2,3]. This newly available technique, i.e., inelastic electron scanning tunneling spectroscopy (IESTS), has a crucial importance since it allows one to spatially visualize the fraction of inelastically scattered electrons by the different vibrational modes of the adsorbate.

It is thus necessary to perform a quantitative calculation of the inelastic images, in order to interpret those obtained experimentally. Despite the fact that there have been several modelistic approaches to the problem [4–8], to our knowledge no calculation of spatially resolved inelastic currents had yet been published. In this paper we want to show how such a calculation can be carried out, and that even a "simple" linear combination of atomic orbitals (LCAO) approach yields a reasonable agreement with experimental results. Our approach permits one to analyze the inelastic current in terms of molecular orbitals. By doing so we are able to give an intuitive interpretation to the in principle "mysterious" fact that the C-H bending modes cannot be detected experimentally.

We will first outline the method to compute inelastic tunneling currents [8,9]. Then we explain the computational details of the present calculation, and afterwards we present and discuss our results, comparing them with the experimental ones.

The inelastic scattering of an electron by the vibrational modes of an adsorbed molecule is described by the Hamiltonian

$$H = \sum_k E_k \hat{C}_k^\dagger \hat{C}_k + \sum_\mu \Omega_\mu \hat{V}_\mu^\dagger \hat{V}_\mu + \sum_\mu (\hat{V}_\mu^\dagger + \hat{V}_\mu) \sum_{ij} \xi_{ij}^{(\mu)} \hat{c}_i^\dagger \hat{c}_j . \quad (1)$$

The inelastic coupling takes place only in a localized group of orbitals, defined by the operators $\hat{c}_i$ and $\hat{c}_i^\dagger$. The coupling of the electron with the vibrational mode μ is given by the ξ's, which are defined as [4]

$$\xi_{ij}^{(\mu)} = \left.\frac{\partial H_{ij}}{\partial R^{(\mu)}}\right|_{R=R_0} \Delta R^{(\mu)}, \quad \Delta R^{(\mu)} = (2m^* \Omega_\mu)^{-1/2} \hbar , \quad (2)$$

where Ω_μ is the energy of the vibrational mode. From here we will assume only one vibrational mode for simplicity, but the extension to the multiple mode case can be made straightforwardly. The inelastic matrix thus defined can be shown to be equivalent to the inelastic coupling elements used in [10] to calculate the vibrational lifetimes of adsorbates due to the electron-hole pair deexcitation mechanism.

The wave function of the electron plus oscillator can be written as

$$|\Phi\rangle = \sum_{n,k} a_{n,k} |\Psi_{n,k}\rangle = \sum_{n,k} a_{n,k} e^{in\Omega t} |ph_n\rangle e^{iE_k t} |\psi_k\rangle , \quad (3)$$

where $|ph_n\rangle$ depends on the phonon coordinates and $|\Psi_k\rangle$ on the electronic ones. The $|\Psi_k\rangle$ describe the propagating eigenfunctions of the electron far from the scatterer. Thus, in the base of $|\psi_{n,k}\rangle$ the Hamiltonian elements are

$$\begin{aligned} H_{nk,n'k'} = {} & \delta_{n,n'} \delta_{k,k'} (E_k + n\Omega) \\ & + (\sqrt{n}\, \delta_{n,n'+1} + \sqrt{n'}\, \delta_{n+1,n'}) \\ & \times \sum_{ij} \langle \psi_k | i \rangle \xi_{ij} \langle j | \psi_k' \rangle \delta(\Omega - E_k + E_k') . \end{aligned} \quad (4)$$

If we now transform to a localized orbital base, the Hamiltonian matrix elements look like

$$\begin{aligned} H_{ni,n'j} = {} & \delta_{n,n'} (H_{ij} + n\Omega\, \delta_{ij}) \\ & + (\sqrt{n}\, \delta_{n,n'+1} + \sqrt{n'}\, \delta_{n+1,n'}) \xi_{ij} . \end{aligned} \quad (5)$$

This is the Hamiltonian of a series of equivalent systems shifted by an energy Ω with respect to the immediate one, and coupled by elements ξ_{ij} at a spatially localized region comprising the adsorbate and its neighboring atoms. This is schematized in Fig. 1.

The fraction of electrons that is inelastically scattered leaving the molecule in its nth excited vibrational level is just the fraction of the current exiting through branch n when it is injected through branch $0'$ in Fig. 1. This

 0031-9007/00/84(16)/3694(4)$15.00 © 2000 The American Physical Society

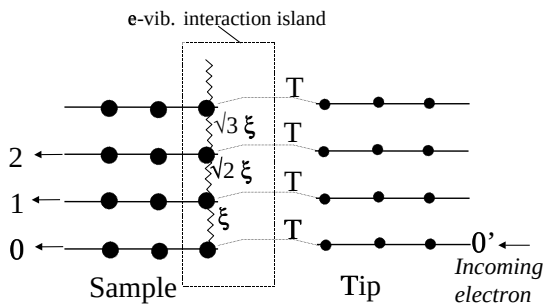

FIG. 1. Schematic representation of the total Hamiltonian in Eq. (5). Each of the horizontal chains corresponds to the electronic Hamiltonian $H_n = H_{\mathrm{el}} + n\Omega I$. They are coupled by the inelastic coupling matrices ξ.

fraction, I_n/I_{total}, is obtained in a Green function approach. In general,

$$I_n = \int_{E_F}^{E_F+eV} \sigma_{0'n}(E)\theta(E - n\Omega_n)\, dE\,, \qquad (6)$$

with the conductances σ being given by [8]

$$\sigma_{0',n} = \frac{8\pi^2 e}{h}\,\mathrm{Tr}[T_t \rho_t(E) T_t^\dagger G_{0n} T_s \rho_s(E - n\Omega) \times T_s^\dagger G_{n0}^*]\,. \qquad (7)$$

Here the matrix G is the total Green function of the coupled system (the indexes n and 0 in general represent groups of many orbitals). The local densities of states ρ_s and ρ_t correspond to the sample and tip "decoupled" electrodes. T_s and T_t are the Hamiltonian matrices coupling the "inelastic island" to the sample and tip electrodes. The experiment in Ref. [3] was shown to be of the "coherent excitation" mechanism type [7]. This means that the deexcitation time of the molecule is much shorter than the mean time between tunneling electrons. Thus we just need to consider the single electron inelastic scattering process, in the way of Eqs. (6) and (7).

We have applied the above formalism to the case of a C_2H_2 molecule adsorbed on Cu(100), in an LCAO approach. The Hamiltonian of the sample was set following the way described in [11]. The hopping matrix elements are those parametrized by Harrison [12]. They are rotated according to the usual Slater-Koster procedure [12]. As in [11], the diagonal matrix elements are taken so as to obtain the orbital levels described in [13]. A Green function "decimation" technique [14] has been used to project the electronic structure of the semi-infinite metal onto the Cu(100) surface atoms. Then, the molecule is coupled to the Cu(100) surface. In the parallel direction, a periodical 3×3 surface cell has been used. Self-consistency has been taken into account by allowing a charge transfer to the molecule, as calculated by [15].

The tip has been modeled in the simplest possible way, in order not to introduce any effects other than the sample properties. Therefore, a tip apex with s-orbital symmetry has been considered. The tip's Green function projected onto its apex has been considered a constant imaginary quantity, so that the local density of states (LDOS) is constant in the whole energy range. An exponential dependence has been assumed for the tip-sample hopping matrix elements. The exponent for the tip-copper elements is such that the conductance vs separation dependence agrees with the potential barrier of the metal surface. Exponents for the hopping elements between the tip and the adsorbate atoms are obtained from the Slater orbitals given in [16]. For the Cu surface we have used a single s-band model. The prefactors for the tip-copper and tip-C matrix elements were determined by a best fit of the calculated elastic image to the experimental STM elastic image. In this way we ensure that the electronic structure of the sample is well described. This completely determines the Hamiltonian, before calculating the inelastic images. Afterwards, the inelastic images just follow straightforwardly from Eq. (7).

Once we have the electronic Hamiltonian, we calculate the inelastic coupling matrices according to Eq. (2), using the experimentally measured frequencies (summarized in Ref. [3]). This has been done for seven different vibrational modes: the C-H stretches, C-C stretch, C-H scissor, C-H wag, C-H twist, and molecule-metal stretch [3]. The inelastic coupling matrix is included to construct the total Hamiltonian of the system, from which we obtain the total Green function. Then we use Eq. (7) to obtain the elastic and inelastic conductance for each of the vibrational modes.

First we show in Fig. 2a the calculated elastic conductance versus the tip's position, $\mathrm{Log}[\sigma_0(x, y)]$, for a 7 Å tip-surface separation. The calculated corrugation is 0.2 Å (the experimental one reported in [3] is 0.3 Å).

We have then calculated the inelastic conductance as a function of the tip's position (Fig. 2b) and the voltage (Fig. 3a). We find a dominance of the C-H stretch mode over the other ones, in agreement with the experimental evidence [2,3]. The calculated profile of $\sigma_{c\text{-hstr}}(x, y)/\sigma_0(x, y)$ is plotted in Fig. 2b, together with the experimental points of [3]. The latter corresponds to "rotation rate" profiles, rather than direct inelastic current measurements, but they can be assumed to be fairly proportional to the inelastic current scattered by the C-H stretch, since this mode is clearly dominant. The profiles have been calculated keeping the tip 7 Å over the surface atoms, starting at the center of the molecule and displacing it laterally in a range of 5 Å, following two perpendicular lines: along the molecule's axis and perpendicular to it. The profile calculated along the axis of the molecule is higher than the one on the perpendicular, in agreement with the experiment. When the tip is laterally displaced 5 Å from the center, the calculated inelastic fraction decreases by 2 orders of magnitude, also in agreement with the experimental profile. The slight bump shape near the center of the molecule is due to a sharp decrease of the elastic conductance (Fig. 2a). This feature is more pronounced in the experiment, what can be attributed to a higher experimental corrugation. The

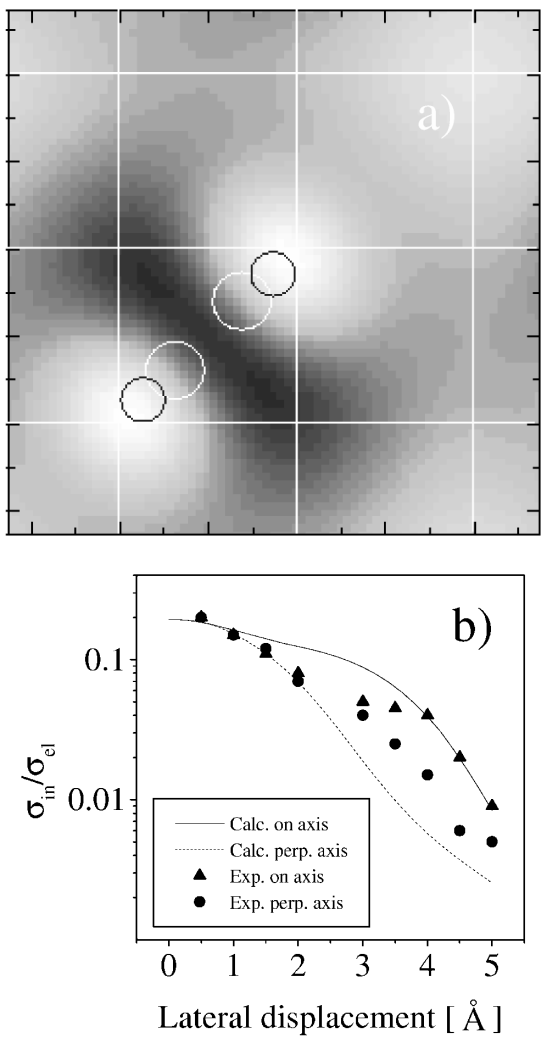

FIG. 2. (a) Calculated constant conductance STM image of the acetylene molecule on Cu(100) (low bias limit, $V \rightarrow 0$). The white lines indicate the surface net, and the circles mark the positions of the molecule's atoms. (b) Calculated inelastic fraction of scattered electrons due to the C-H stretching vibrational modes plotted as a function of the tip's lateral displacement (parallel to the surface), for electrons with $E = E_F^{\text{sample}}$, and experimental results from [3]. The 0 displacement corresponds to the tip located over the center of the molecule. Solid line (calculated) and circles (expt.): profile along the axis of the molecule. Dotted line (calc.) and triangles (expt.): profile along the line perpendicular to the molecule's axis.

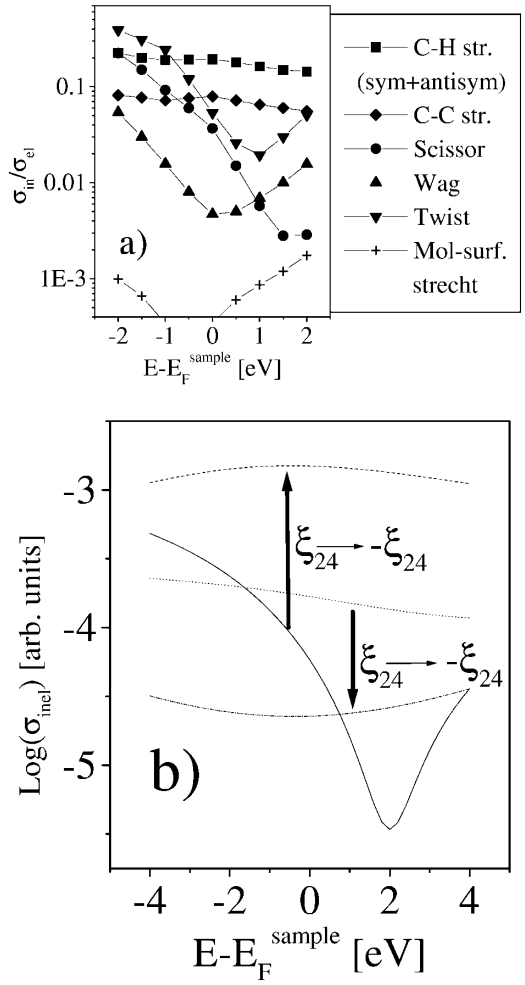

FIG. 3. (a) Dependence of the inelastic conductance for the different modes as a function of the electron's energy. The tip is located over the center of the molecule. The inelastic conductance has been normalized by the elastic one at the same energy. The elastic conductance at this tip's position keeps quite constant along the energy range, changing just by about a factor of 2. (b) Interference effect in the case of the C-H symmetric stretching mode and the C-H scissor mode. In the case of the stretching mode, the inelastic scattering through orbitals $2a_1$ and $5a_1$ interferes constructively (solid line). The interference becomes destructive if we change the sign of ξ_{24} and ξ_{42} in the inelastic scattering matrix (dashed line). Similarly, the destructive interference in the case of the C-H scissor mode (dash-dotted line) becomes constructive when $\xi_{24} \rightarrow -\xi_{24}$ (dotted line).

calculated value of $\sigma_{c\text{-hstr}}/\sigma_{\text{elast}}$ is about 20% (about 15% of the total conductance). The fractions experimentally measured by STM inelastic electron-tunneling spectrosocpy (STM-IETS) are very much tip dependent, and oscillate between 6% and 12%, being of the same order of magnitude as our result.

The profiles calculated for other modes are smaller than the C-H stretch for the experimental range of energies (as shown in Fig. 3a). Near the center of the molecule, the C-C stretching mode's inelastic fraction is 0.3 times that of the C-H stretch. This ratio might be an overestimation, being the real ratio smaller, since a 0.3 would in principle allow the STM-IETS detection of the C-C mode. A more refined Hamiltonian going beyond Harrison's matrix elements might give a smaller ratio. Nevertheless, one would not expect a significant difference regarding the order of magnitude.

The clear dominance of the C-H stretch over the C-H bending modes in the inelastic scattering of electrons is a quite striking fact. The greater the frequency the smaller the mean displacement, what implies a smaller inelastic coupling according to Eq. (2). This argument would thus oppose both the experimental and the calculated evidence. In fact, the absolute values of the calculated

inelastic coupling matrix elements are of the same order of magnitude for the stretching and bending modes, being even bigger in the latter case. If we now look at the voltage behavior of the inelastic fractions of the conductance, $\sigma_{\mathrm{inel}}(E)/\sigma_{\mathrm{total}}(E)$ we find a markedly different behavior between the modes: while the stretching mode contribution keeps quite constant in a range of several eV, the bending modes present a deep decrease near the center of the graph, and grow even higher than the C-H stretch contribution at high biases. These facts indicate that interference between several orbitals is taking place in the inelastic conduction process.

To illustrate this we will compare the symmetric bending mode (scissor) with the symmetric C-H stretching mode. Since these are symmetric modes, they do not mix electrons from states with odd symmetry. The tip is on top of the molecule, so only electrons of even symmetry can tunnel. Therefore, we can forget about all the odd symmetry electrons in the problem, and consider just the four symmetric molecular orbitals ($2a_1, 3a_1, \sigma_\pi$, and $5a_1$; at subindexes we will denote them by 2, 3, 4, and 5, respectively). From those orbitals, only one (the highest occupied molecular orbital, denoted σ_π by Hoffman [13]) has an appreciable density of states at the Fermi level. Thus only this orbital carries current elastically to the tip. However, the inelastic process takes place at more than just this orbital. Otherwise the inelastic fractions due to the two modes would be exactly proportional by $\xi_{\mathrm{sciss}}/\xi_{\mathrm{str}}$, which is not the case. Furthermore, the inelastic matrix element for the σ_π orbital in the scissor mode turns out to be bigger than that in the symmetrical stretching mode. These considerations imply that there is interference between several orbitals in the inelastic conduction process.

Even after simplifying the problem to a 4 orbital one (the Cu atoms affect very little to the inelastic current), the analysis is still not trivial, since the $\xi_{i,j}$ matrix has a dimension of 16×16. Nevertheless, only the elements ξ_{i,σ_π} are important. This can be proven by use of Eq. (7) and the fact that the three orbitals other than σ_π have a much smaller LDOS at the Fermi level than the latter. Thus the analysis reduces to a comparison of only four numbers for the two modes.

From these four elements, the bigger ones are $\xi_{2,4}$ and $\xi_{5,4}$. Now, $\mathrm{sgn}[\xi_{2,4}^{\mathrm{str}}] = -\mathrm{sgn}[\xi_{5,4}^{\mathrm{str}}]$, while $\mathrm{sgn}[\xi_{2,4}^{\mathrm{sciss}}] = \mathrm{sgn}[\xi_{5,4}^{\mathrm{sciss}}]$. This qualitative difference results in a constructive interference in the stretch case and a destructive one in the scissor case. To prove that this is so, we have changed the sign of $\xi_{5,4}$ in the two cases, obtaining the curves shown in Fig. 3b. It is clear how the qualitative behavior of the two modes is exchanged: now the stretching mode inelastic fraction is smaller and shows a decrease in the middle of the graph, while the scissor mode increases at that region, and shows a much bigger value, being the dominating one. Further analysis shows similar interferences taking place for the other bending modes.

The geometrical origin of the relative signs arises simply from the fact that (1) *the stretching mode affects more strongly the hopping between the s orbitals at H and C, while* (2) *the scissor mode affects that between the hydrogen s orbital and the carbon p orbital taken perpendicular to the bond direction*. The relative signs of the molecular wave function at these atomic orbitals differ between the $2a_1$ and $5a_1$ for the first case, and coincides for the second case, originating the sign relations in ξ discussed before.

We have shown how to calculate inelastic images of adsorbed molecules, and have compared with the experimental ones in the case of an acetylene molecule on Cu(100). A dominance of the C-H stretch mode over the other modes has been obtained, in accordance with experimental evidence. The calculated inelastic profiles are in good qualitative agreement with those reported experimentally. As a function of the bias, two qualitatively different behaviors have been obtained for the C-H stretching and bending modes. This difference has been shown to correspond to an interference phenomenon in the inelastic scattering process, and is believed to be the reason why the bending modes have not been detected experimentally.

We acknowledge W. Ho, M. Rose, M. Salmeron, R. Perez, and F. Flores for helpful comments.

*Present address: NASA-Ames Research Center, Mail Stop 27A-1, Moffett Field, CA 94035.

[1] R. C. Jaklevic and J. Lambe, Phys. Rev. Lett. **17**, 1139 (1966).
[2] B. C. Stipe, M. A. Rezaei, and W. Ho, Science **280**, 1732 (1998); Phys. Rev. Lett. **82**, 1724 (1999), and references therein.
[3] B. C. Stipe, M. A. Rezaei, and W. Ho, Phys. Rev. Lett. **81**, 1263 (1998).
[4] B. N. J. Persson and A. Baratoff, Phys. Rev. Lett. **59**, 339 (1987).
[5] M. A. Gata and P. R. Antoniewicz, Phys. Rev. B **47**, 13 797 (1993).
[6] K. Stokbro, Ben Yu-Kuang Hu, C. Thirstrup, and X. C. Xie, Phys. Rev. B **58**, 8038 (1998).
[7] G. P. Salam, M. Persson, and R. E. Palmer, Phys. Rev. B **49**, 10 655 (1994).
[8] N. Mingo and K. Makoshi, Surf. Sci. **438**, 261–270 (1999).
[9] N. Mingo and K. Makoshi, "Proceedings of ACSIN 1999" (to be published).
[10] M. Head-Gordon and J. C. Tully, J. Chem. Phys. **96**, 3939 (1992).
[11] B. Hellsing, Surf. Sci. **282**, 216 (1993).
[12] W. A. Harrison, *Electronic Structure and the Properties of Solids* (Freeman, New York, 1980).
[13] D. M. Hoffman, R. Hoffmann, and R. Fisel, J. Am. Chem. Soc. **104**, 3858 (1982).
[14] F. Guinea, C. Tejedor, F. Flores, and E. Louis, Phys. Rev. B **28**, 4397 (1983).
[15] S. Hengrasmee and J. B. Peel, Surf. Sci. **184**, 434 (1987).
[16] J. Silvestre and R. Hoffmann, Langmuir **1**, 621 (1985).